JOURNAL OF MATERIALS SCIENCE 22 (1987) 871–876

Role of crack size in the bi-modal static fatigue failure of a cordierite glass and glass–ceramic

SURESH BASKARAN, HONG LIM LEE*, D. P. H. HASSELMAN
Department of Materials Engineering, Virginia Polytechnic Institute and State University, Blacksburg, Virginia 24061, USA

A study was conducted of the static fatigue behaviour at room temperature of a cordierite glass and glass–ceramic with model flaws of two different sizes introduced by the indentation fracture method. For the cordierite glass the stress intensity exponent, N, for sub-critical crack growth inferred from the dependence of time-to-failure on stress was the same for the two different crack sizes and showed good agreement with the value of N for data obtained in an earlier study for dynamic fatigue and by the double-torsion method. For the cordierite glass–ceramic, which consisted of larger crystallites (a few micrometres in size) embedded in a primarily crystalline fine-grained matrix, the static fatigue response depended strongly on crack size, also observed during dynamic fatigue. This effect was attributed to the relative size difference between the cracks and the crystallites. The small cracks could propagate in a planar fashion, whereas the larger cracks were subject to toughening by crack-deflection around the crystallites and a corresponding decrease in the rate of sub-critical crack growth. An analysis for the case of idealized "bi-modal" crack-size dependent sub-critical crack-growth indicated that, for a cordierite glass–ceramic with small cracks, the role of the larger crystallites serves to introduce a "pseudo" fatigue-limit.

1. Introduction

Particulate continuous-phase brittle ceramic composites such as ceramic–ceramic [1] and glass–crystal [2–6] composites as well as glass–ceramics [7–12] can exhibit mechanical properties such as fracture toughness and strength superior to those of single-phase brittle materials. Such improvements in mechanical behaviour are the direct result of the interaction between the propagating crack and the dispersed phase. Such interaction in the form of crack-bowing [13, 14] between or crack-deflection [15–17] around second-phase dispersions can lead to significant increases in fracture toughness. A similar effect can also arise from stress-induced micro-cracking [18, 19]. Non-uniform stress distributions near the dispersions due to mismatches in coefficients of thermal expansion and elastic moduli also can play a significant role in affecting the path of crack propagation [20, 21]. Second-phase dispersions can also effectively reduce the rise of failure-initiating flaws introduced during surface preparation [3]. This latter effect, coupled with a corresponding increase in fracture toughness, can serve to increase strength considerably.

The contributions of a number of these effects to mechanical behaviour were the subject of earlier investigations [12, 22] which concentrated on a series of cordierite glass–ceramics as well as the original glass with the aid of specimens with model surface flaws introduced by Vickers indentations. Generally, it was found that the mechanical properties of the cordierite in the glassy state, such as fracture toughness and strain-rate sensitivity, were independent of indentation load and associated crack size. However, for the glass–ceramic, which consisted of larger crystallites with a size of a few micrometres embedded in a nearly crystalline fine-grained ($\sim 0.1\,\mu m$) matrix, significant differences in mechanical properties for different crack sizes were found. Over an intermediate range of indentation load referred to as the "transition" region and associated "transition" crack size, a_t, the radial crack size was found to be a constant, as the result of crack-pinning at the larger crystallites. At this transition crack size the fracture toughness showed a discontinuous increase. Furthermore, other mechanical properties such as inert strength and strain-rate sensitivity in aqueous environment showed significant differences for initial crack sizes either smaller or larger than a_t. In this respect, differences in observed strain-rate sensitivity and that predicted from data for sub-critical crack growth were also noted by other investigators [23, 24].

The purpose of the present study was to investigate the crack-size dependence of the static fatigue (i.e. constant stress) behaviour of the cordierite glass and glass–ceramics.

2. Experimental procedure

2.1. Materials and specimen preparation

The cordierite glass and glass–ceramic chosen for this study were identical to those used in earlier

*On sabbatical leave from Department of Ceramic Engineering, Yonsei University, Seoul, Korea.

0022–2461/87 $03.00 + .12

investigations [12, 22, 25]. All specimens were obtained from the same block of the original glass* used for the study of the effect of crack size on strain-rate sensitivity. The materials of this study consisted of the original glass and the glass–ceramic obtained by a heat-treatment which consisted of a nucleation stage of 2 h at 820° C followed by crystallite growth for 8 h at 1260° C. The microstructure for the glass–ceramic made by this heating schedule was presented earlier [22].

The specimens for the measurement of static-fatigue behaviour were in the form of thin circular discs 1.25 cm in diameter and approx ~ 1 mm thick. These specimens were cut with a slow-speed diamond saw from 1.25 cm circular cylinders, which were heat-treated following diamond core-drilling from the block of the original glass. The surface of the specimen to be subjected to the tensile stress was ground and polished using 600 grit SiC, 1 μm Al_2O_3 and finally 0.25 μm diamond paste. Following polishing, the specimens were annealed for 3 h at 600° C to remove possible surface stresses introduced during cutting and polishing. The thickness of the specimens following polishing was held to an accuracy of 1.00 $\pm$ 0.01 mm, in order to minimize the effect of stress-gradient and other specimen-size dependent effects on the experimental results. Following the anneal, the surface was etched with a 5% aqueous solution of HF for 30 sec in order to eliminate or reduce the effectiveness of any inherent surface flaws or other damage caused by and not removed during surface preparation. These surfaces were then indented with a single Vickers-diamond indentation at the exact centre of the specimen. The cordierite glass specimens were indented with loads of 1.96 and 4.9 N, which resulted in mean crack sizes of 25 and 49 μm, respectively, as measured from the centre of the indentation to the crack tip. The cordierite glass–ceramic specimens were idented with loads of 0.98 and 9.8 N, which yielded crack sizes of 12.5 and 53 μm, respectively. The values of these loads were chosen such that at the lower value of load, as indicated by the earlier findings [12, 22], the cracks were small enough to fit within and have their crack-propagation controlled by the fine-grained matrix. At the higher value of load of 9.8 N, the crack size was sufficiently high that its propagation required interaction with the larger crystallites, primarily in the form of crack deflection.

2.2. Static fatigue tests

The circular disc specimens as described above were subjected to biaxial flexure as described by Wachtman *et al.* [26]. The specimen, covered with deionized water, was placed in an appropriate specimen holder and concentrically supported on three ball-bearings with diameter of 1.6 mm evenly spaced around a circle with radius of 3.57 mm. All tests were conducted at room temperature. The specimen was loaded by means of a compressive load transmitted through a concentrically located right circular cylinder with a diameter of 1.6 mm, which, in turn, was loaded by a hinged moment arm with movable weight, which allowed variation of the load applied to the specimen. The moment arm was equipped with an electronic counter which automatically recorded the time period to failure at a given value of stress. From the value of load the maximum tensile stress (σ) in the surface of the specimen was calculated from [26]

$$\sigma = \frac{3P}{4\pi t^2}(1 + \nu)\left[1 + 2\ln\left(\frac{a}{b}\right) + \left(\frac{1 - \nu}{1 + \nu}\right)\left(\frac{1 - b^2}{2a^2}\right)\frac{a^2}{R^2}\right] \quad (1)$$

where P is the breaking load of the sample, b is the radius of the piston pin, a is the radius of the ball-bearing support circle, and ν, t and R are Poisson's ratio, the specimen thickness, and radius of the sample, respectively. For the calculation of the stress, Poisson's ratio was taken to be equal to 0.25.

For purposes of analysis of the data, it was assumed that the rate of sub-critical crack growth, V, as a function of the Mode I stress intensity factor, K_I, could be expressed by [27]

$$V = AK_I^N \quad (2)$$

From Equation 2 the time-to-failure, t_f, at a level of applied stress, σ_a well below the instantaneous fracture stress, σ_i, can be derived to be [28]

$$t = B\sigma_i^{N-2}\sigma_a^{-N} \quad (3)$$

where B is a constant.

Equation 3 indicates that the slope of the $\ln\sigma_a$ against $\ln t_f$ plot should be N^{-1}. For indentation cracks, however, the rate of crack growth is affected by the residual stress field around the indentation. As shown by Fuller *et al* [29], the exponent N in Equation 2 can be obtained from the reciprocal slope N_1 of the $\ln\sigma_a$ against $\ln t_f$ plot for indentation cracks from

$$N = \frac{4N_1}{3} - \frac{2}{3} \quad (4)$$

3. Results, discussion, analysis and conclusions

Figs 1 and 2 in the form of double logarithmic plots show the experimental data for the dependence of stress (σ_a) on time-to-failure (t_f) for the cordierite glass and glass–ceramic specimens, respectively. Table I summarizes the values of indentation load, mean crack size and corresponding values of the slope of the $\ln(\sigma_a)$–$\ln(t_f)$ plots and the corresponding values of the exponent N. The two sets of cordierite glass specimens with the two different values of mean crack size exhibit almost identical values of N of 37 and 38. The values are somewhat less than the value of 46 found for the strain-rate sensitivity for specimens with a mean crack size of 24.9 μm [22], but compare very favourably with two values of N of 32.1 and 37.6 measured directly [22] by the double-torsion method. This relatively good agreement between the values of

*Corning Glass Works C9604. This glass when crystallized following commercial heat treatment practice results in the glass–ceramic designated C-9606.

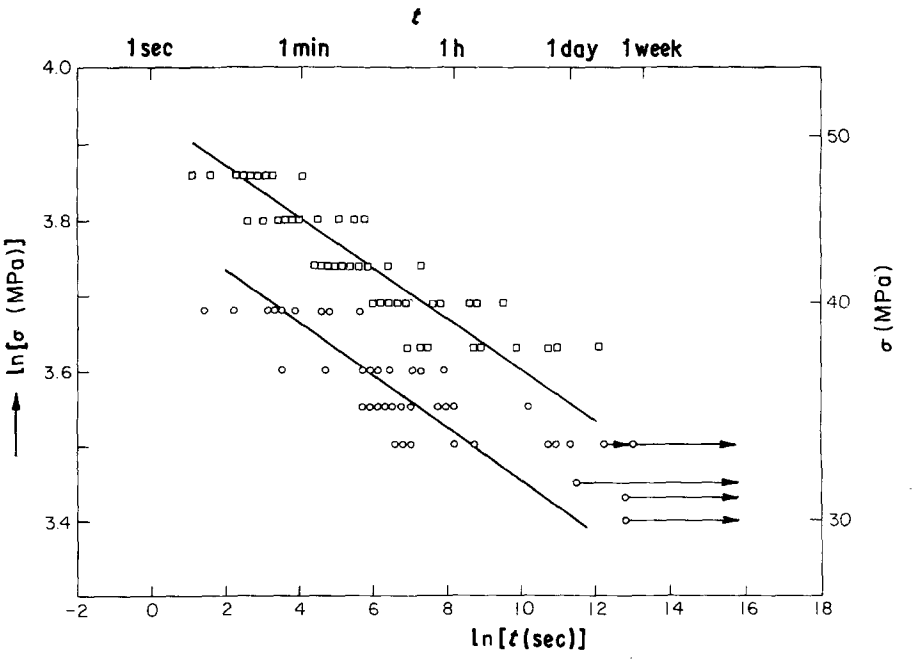

Figure 1 Stress dependence of static-fatigue life of cordierite glass with indentation cracks with different initial size. (Arrows indicate specimens which had not failed at the indicated time.) Mean crack size (□) 24.9 μm, (○) 48.5 μm.

N suggests that for the glass, sub-critical crack growth for large cracks in the double-torsion test, and for small cracks under conditions of static and dynamic fatigue, is governed by the same mechanism.

In contrast, the fatigue behaviour of the cordierite glass–ceramic specimen with the two different values of crack size appears to differ significantly. The values of N of 34 and 121 for the mean crack sizes of 12.5 and 53.0 μm, respectively, must be considered significantly different, which implies that the sub-critical growths of these two crack sizes appear to be governed by different mechanisms. The value of N of 34 for the mean crack size of 12.5 μm compares favourably with the value of 39 found for the strain-rate sensitivity for identical specimens found earlier [22]. For the specimens with mean crack size of 53.0 μm, the value of $N = 121$ for static fatigue as found in this study is identical to the value of 121 for the strain-rate sensitivity and only slightly higher than the values of 93.5 and 99 obtained by the double-torsion technique [22]. The good agreement for the values of N obtained by different techniques serves to confirm the earlier conclusion that in the cordierite glass–ceramic small- and large-sized cracks can exhibit significantly different propagation characteristics, as the direct result of the presence or absence of interactions between the propagating crack and the larger crystallites contained within the fine-grained matrix [22].

An interesting speculation can be made about the stress dependence of the static fatigue behaviour of the cordierite glass–ceramic specimens for times-to-failure larger than those for this study, which extended over periods up to about three days. A direct linear extrapolation of the data in Fig. 2 to lower stress values is inappropriate, as at the same value of stress the fatigue-life of the specimens with small cracks would be less than the fatigue-life of the specimens with the larger cracks. Clearly, account needs to be taken of the transition in the kinetics of sub-critical crack growth, when the size of the initially small cracks reaches the "transition" crack size, a_t. When the latter condition is obtained, the stress dependence of fatigue-life should exhibit some form of discontinuity. The nature of this discontinuity can be analysed as follows.

It will be assumed, for simplicity, that the rate of sub-critical crack growth is affected by the applied stress only. In this manner, the analysis to be presented can follow the original approach of Ritter [28]. The effect of other stresses such as those due to thermal expansion mismatches or residual stress fields around indentation cracks can be included by the method of Fuller *et al.* [29].

The fracture toughness (K_{Ic}) and sub-critical crack growth for crack sizes below and above the transition crack size exhibit bi-model behaviour as shown schematically in Fig. 3, and will be described by

$$K_{Ic} = K'_{Ic} \quad \text{and} \quad V = A'K_I^N \quad \text{for } a < a_t \tag{5}$$

TABLE I Indentation load, crack size, slope of fatigue curve and crack growth exponent for static fatigue behaviour of indented cordierite glass and glass–ceramic.

Materials	Indentation load (N)	Crack size (μm)	Slope of $\log(\sigma_f)$ against $\log(t)$	Crack growth exponent, N
Cordierite glass (as received)	1.96	24.9 ± 3.0	0.034 ± 0.003†	38
	4.90	48.5 ± 4.7	0.035 ± 0.004	37
Cordierite glass–ceramic*	0.98	12.5 ± 1.1	0.039 ± 0.004	34
	9.80	53.0 ± 4.2	0.011 ± 0.001	121

*Crystallized at 1260° C for 8 h, following nucleation at 820° C for 2 h.
†Standard deviation.

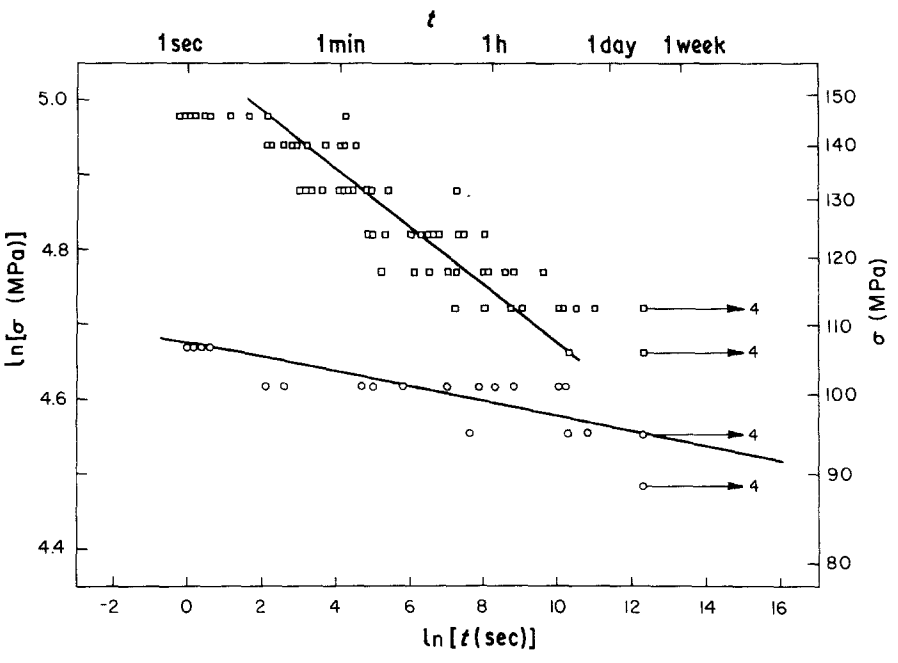

Figure 2 Stress dependence of static-fatigue life of cordierite glass–ceramic with indentation cracks with different initial size. (Arrows and numbers indicates specimens which had not failed at the indicated time). Mean crack size (□) 12.5 μm, (○) 53.0 μm.

$$K_{Ic} = K''_{Ic} \quad \text{and} \quad V = A''K_I^{N''} \quad \text{for } a > a_t \tag{6}$$

For purposes of the analysis two values of the fracture stress (σ_f) will be defined:

$$\sigma'_f = K'_{Ic}/Ya^{1/2} \quad \text{for } a < a_t \tag{7}$$

and

$$\sigma''_f = K''_{Ic}/Ya^{1/2} \quad \text{for } a > a_t \tag{8}$$

where Y is a constant related to the crack geometry and stress distribution.

At the transition crack size, a_t, the fracture stresses defined by Equations 7 and 8 become

$$\sigma' = K'_{Ic}/Ya_t^{1/2} \tag{9}$$

and

$$\sigma''_t = K''_{Ic}/Ya_t^{1/2} \tag{10}$$

Due to the bi-modal behaviour as described above, three distinctly different situations must be considered in the analysis of fatigue-life. For an initial crack size $a_i < a_t$, and a sufficiently high stress level $\sigma > \sigma'_t$, such that the crack becomes critical at a final crack size $a_f < a_t$, sub-critical crack growth over the total fatigue life is described by Equation 5. Similarly, for an initial crack size $a_i > a_t$, fatigue-life will be governed by Equation 6.

A more complex situation is encountered for an initial crack size $a_i < a_t$, which at a sufficiently low stress level does not reach the conditions of criticality when $a = a_t$. In this case, the initial stages of fatigue-life will be described by Equation 5, whereas the subsequent stages of fatigue-life are governed by sub-critical crack growth expressed by Equation 6.

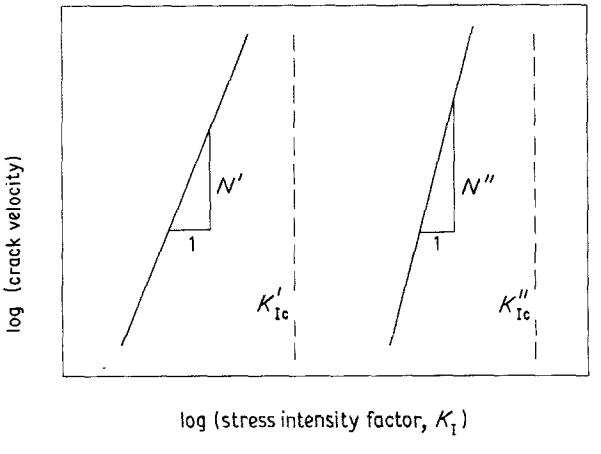

Figure 3 Idealized bi-model sub-critical growth of cracks in glass–ceramic subject to different mechanisms for small cracks (left) and large cracks (right).

An expression for the time-to-failure (t_f) measured from the instant of time, $t = 0$, at which the load is applied can be derived on the basis of well-known fracture-mechanical principles [27]. With the aid of the general equation which relates the stress intensity factor, K, the stress, σ, and the crack size, a,

$$K = \sigma Ya^{1/2} \tag{11}$$

Equation 2 for the rate of sub-critical crack growth $V = da/dt$ can be written

$$da = A\sigma^N Y^N a^{N/2}\, dt \tag{12}$$

from which the time-to-failure (t_f) can be derived to be

$$t_f = \frac{2}{(N-2)AY^N\sigma^N}\left[a_i^{-(N-2)/2} - a_f^{-(N-2)/2}\right] \tag{13}$$

where a_f is the final crack length at which $K_I = K_{Ic}$.

Usually, $N \gg 1$ such that

$$a_f^{-(N-2)/2} \ll a_i^{-(N-2)/2} \tag{14}$$

which permits Equation 13 to be simplified to

$$t_f = \frac{2a_i^{-(N-2)/2}}{(N-2)AY^N\sigma^N} \tag{15}$$

With the aid of Equations 11 or 13 expressions can be obtained for the three situations of fatigue-failure

due to the bi-modal behaviour described above. For simplicity, the simplifying assumption described by Equation 14 in order to obtain Equation 15 will be assumed to be valid throughout.

The failure-times for the three situations with the aid of Equation 13 can be written as follows:

(a) For values of stress and initial crack size, such that

$$\sigma > \sigma_t' \quad \text{and} \quad a_i < a_t \tag{16}$$

crack growth and fracture will be governed entirely by Equations 5 and 7, so that Equation 15 for the time-to-failure, t_f', becomes

$$t_f' = \frac{2a_i^{-(N'-2)/2}}{(N'-2)A'Y^{N'}\sigma^{N'}} \tag{17}$$

(b) For values of stress and initial crack size, such that

$$\sigma < \sigma_t'' \quad \text{and} \quad a_i > a_t \tag{18}$$

crack growth and fracture will be governed entirely by Equations 6 and 8, so that Equation 15 for the time-to-failure, t_f'', becomes

$$t_f'' = \frac{2a_i^{-(N''-2)/2}}{(N''-2)A''Y^{N''}\sigma^{N''}} \tag{19}$$

(c) For values of stress and initial crack size, such that

$$\sigma < \sigma_t' \quad \text{and} \quad a_i < a_t \tag{20}$$

crack growth is governed by both Equations 5 and 6, and fracture governed by Equation 8. For these conditions, the total time-to-failure is the sum of the time periods required for the crack to grow from the initial crack size a_i to the transition crack size a_t, and from the latter size to the size, a_f, at which the failure criterion of Equation 8 is satisfied.

Assuming that $a_i \ll a_t$ and $a_t \ll a_f$ so that the simplification of Equation 14 remains valid, the total time-to-failure from Equation 15 becomes

$$t_{ft} = t_f' + t_f'' = \frac{2a_i^{(N'-2)/2}}{(N'-2)A'Y^{N'}\sigma^{N'}} + \frac{2a_t^{-(N''-2)/2}}{(N''-2)A''Y^{N''}\sigma^{N''}} \tag{21}$$

An interesting situation arises at a stress level $\sigma < \sigma_t'$, at which a crack with initial size $a_i < a_t$ will be just short of becoming critical when its size equals a_t. Because of the bi-modal change in crack growth characteristics, it again will be highly sub-critical for $a > a_t$. For this reason, at the stress level σ_t', no failure will occur over the period of time required for the crack to grow from the transition crack size a_t to the final size a_f, at which the fracture criterion of Equation 8 is satisfied.

At the value of stress $\sigma = \sigma_t$, the period of time over which no fatigue failure will occur is given by the second term of Equation 21 with σ replaced by σ_t, which yields

$$\Delta t_f = \frac{2a_t^{-(N''-2)/2}}{(N'-2)A''Y^{N''}\sigma_t^{N''}} \tag{22}$$

The stress dependence of the failure time as predicted by Equations 17, 19, 21 and 22 is depicted schematically in Fig. 4. As shown, fatigue life as a function of stress for a material with bi-modal crack growth characteristics is divided into an upper branch which corresponds to high stress ($\sigma > \sigma_t$) and small crack size ($a_i < a_t$), and a lower branch which corresponds to lower values of stress ($\sigma < \sigma_t$) and large crack sizes ($a_i > a_t$). At the level of the transition stress, σ_t, the fatigue data for $a_i < a_t$ should show a discontinuity in magnitude. Also, if N' and N'' are not the same, a discontinuity in slope should be expected as well.

In regard to the results of this study, it is suggested that the fatigue data shown in Fig. 2, for the specimens with mean crack size of 12.5 μm, correspond to the upper curve shown in Fig. 4, whereas the data for the specimens with initial crack size of 53 μm correspond to the lower branch.

An estimate for the time-period Δt_f of Equation 22 can be made for the cordierite glass–ceramic specimens of this study. The data for the sub-critical crack growth behaviour measured by the double-torsion method indicate that the crack velocity, V, at room temperature in water can be expressed by [26]

$$V = 10^{-608}K_I^{96.3} \quad \text{(in SI units)} \tag{23}$$

so that the quantities A'' and N'' in Equation 22 equal 10^{-608} and 96.3, respectively.

The dimension of the transition crack, a_t, as measured from the centre of the indentation to the crack tip as indicated by the data of Morena *et al* [12] equals $\approx 20 \times 10^{-6}$ m.

Because of the uncertainty in the geometry of the surface cracks, which are thought [12, 22, 25] to be in the Palmqvist crack configuration [30–34], the constant Y (Equation 11) was determined indirectly from the values of the fracture stress and fracture toughness [12] of ~ 280 MPa and 2.2 MN m$^{-3/2}$ respectively, which with the aid of Equation 11 yields $Y \sim 3.6$.

The level of stress, σ_t, at which a transition crack of size $a_t = 20 \times 10^{-6}$ m will just be short of being unstable can be calculated from the value of fracture toughness for $a < a_t$ found by Morena *et al.* [25] to be ~ 1.7 MN m$^{-3/2}$, which with the aid of Equation 11 yields $\sigma \sim 105$ MPa.

Substitution of the above values of A'', N'', Y, a_t and σ_t into Equation 22 yields

$$\Delta t_f \approx 10^{48} \text{ sec} \tag{24}$$

This value of t_f implies that for all practical purposes for $a_t \leqslant 20 \times 10^{-6}$ m and $\sigma_t \leqslant 105$ MPa no failure will occur in this cordierite glass–ceramic at room temperature in water. Because of the long time-period required, experimental verification of these latter conclusions at room temperature appears impractical.

Regardless of the quantitative aspects, the existence of a time interval over which no fatigue-failure will occur suggests that the presence of the crystallites in the cordierite glass–ceramic of this study in effect serves to introduce a "pseudo-fatigue" limit. It is speculated that such bi-modal fatigue behaviour and

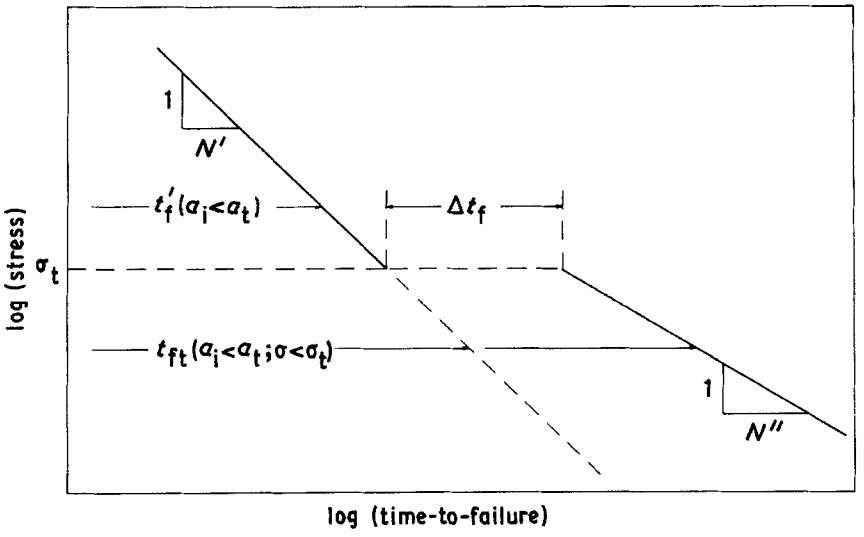

Figure 4 Schematic stress dependence of static-fatigue behaviour of glass–ceramic subject to bimodal sub-critical crack growth.

associated pseudo-fatigue limit, as analysed above, may be exhibited not only by glass–ceramic materials but also by other particulate-, whisker-, or fibre-reinforced brittle matrix composites, in which the failure initiating flaw initially is free to propagate through the matrix phase only, followed by a significant reduction in the rate of sub-critical growth once it has reached a size at which its continued propagation is affected by the reinforcing agent.

In summary, the results of this study have shown that compared to the original glass the crystallites in cordierite glass–ceramics serve to significantly increase static fatigue resistance, with different behaviour for small and large cracks.

Acknowledgements

This study was supported by the Office of Basic Energy Sciences, Department of Energy, under contract No. DE-A505-82ER- 10937. During his sabbatical leave, Professor Lee was supported in part by a grant provided by the Exxon Foundation. Special appreciation is extended to Corning Glass Works, who provided a block of the cordierite glass for this study.

References

1. F. F. LANGE, in "Composite Materials", Vol. 5, Fracture and Fatigue, edited by L. J. Broutman (Academic Press, New York, London, 1974) p. 2.
2. D. B. BINNS, in "Science of Ceramics", Vol. 1, edited by G. H. Stewart (Academic Press, New York, 1962) p. 315.
3. D. P. H. HASSELMAN and R. M. FULRATH, *J. Amer. Ceram. Soc.* **49** (1966) 68.
4. W. J. FREY and J. D. MACKENZIE, *J. Mater. Sci.* **2** (1967) 124.
5. F. F. LANGE, *J. Amer. Ceram. Soc.* **54** (1971) 614.
6. J. C. SWEARINGEN, E. K. BEAUCHAMP and R. J. EAGEN, in "Fracture Mechanics of Ceramics", Vol. 4, Crack Growth and Microstructure, edited by R. C. Bradt, D. P. H. Hasselman and F. F. Lange (Plenum, New York, 1978) p. 973.
7. S. W. FREIMAN and L. L. HENCH, *J. Amer. Ceram. Soc.* **55** (1972) 86.
8. P. HING and P. W. McMILLAN, *J. Mater. Sci.* **8** (1973) 1041.
9. S. W. FREIMAN, G. Y. ONODA Jr and A. G. PINCUS, *J. Amer. Ceram. Soc.* **57** (1974) 8.
10. D. I. H. ATKINSON and P. W. McMILLAN, *J. Mater. Sci.* **11** (1976) 989.
11. C. J. FAIRBANKS, H. L. LEE and D. P. H. HASSELMAN, *J. Amer. Ceram. Soc.* **67** (1984) 236.
12. R. MORENA, K. NIIHARA and D. P. H. HASSELMAN, *Ibid.* **66** (1983) 673.
13. F. F. LANGE, *Phil. Mag.* **22** (1970) 983.
14. A. G. EVANS, *ibid.* **26** (1972) 1327.
15. K. T. FABER, A. G. EVANS and M. D. DRORY, in "Fracture Mechanics of Ceramics", Vol. 6, edited by R. C. Bradt, A. G. Evans, D. P. H. Hasselman and F. F. Lange (Plenum, New York, 1983) p. 77.
16. K. T. FABER and A. G. EVANS, *Acta Metall.* **31** (1983) 565.
17. *Idem, ibid.* **31** (1983) 577.
18. A. G. EVANS and K. T. FABER, *J. Amer. Ceram. Soc.* **64** (1981) 394.
19. *Idem, ibid.* **67** (1984) 255.
20. A. K. KHAUND, V. D. KRSTIC and P. S. NICHOLSON, *J. Mater. Sci.* **12** (1977) 2269.
21. M. P. BOROM, *J. Amer. Ceram. Soc.* **60** (1977) 17.
22. S. BASKARAN, S. B. BHADURI and D. P. H. HASSELMAN, *ibid.* **68** (1985) 112.
23. B. J. PLETKA and S. M. WIEDERHORN, *J. Mater. Sci.* **17** (1982) 1247.
24. T. E. ADAMS, D. J. LANDINI, C. A. SCHUMACHER and R. C. BRADT, *Amer. Ceram. Soc. Bull.* **60** (1981) 730.
25. R. MORENA, K. NIIHARA and D. P. H HASSELMAN, in "Fracture Mechanics of Ceramics", Vol. 5, edited by R. C. Bradt, A. G. Evans, D. P. H. Hasselman and F. F. Lange (Plenum, New York, 1983) p. 145.
26. J. B. WACHTMAN Jr, W. CAPPS and J. MANDEL, *J. Mater.* **7** (1972) 188.
27. R. C. BRADT, A. G. EVANS, D. P. H. HASSELMAN and F. F. LANGE. (eds), "Fracture Mechanics of Ceramics", Vols. 1 to 6 (Plenum, New York, 1974, 1978, 1983).
28. J. E. RITTER Jr, in "Fracture Mechanics of Ceramics", Vol. 4, edited by R. C. Bradt, D. P. H. Hasselman and F. F. Lange (Plenum, New York, 1974) p. 667.
29. E. R. FULLER, B. R. LAWN and R. F. COOK, *J. Amer. Ceram. Soc.* **65** (1983) 314.
30. S. PALMQVIST, *Arch. Eisenhuettenwesen* **33** (1962) 629.
31. I. M. OGILVY, C. M. PERROT and J. W. SUITER, *Wear* **43** (1977) 239.
32. J. T. HAGAN and M. V. SWAIN, *J. Phys. D: Appl. Phys.* **11** (1978) 2091.
33. K. NIIHARA, R. MORENA and D. P. H. HASSELMAN, in "Fracture Mechanics of Ceramics", Vol. 5, edited by R. C. Bradt, A. G. Evans, D. P. H. Hasselman and F. F. Lange (Plenum, New York, 1983) p. 97.
34. D. K. SHETTY, I. G. WRIGHT, P. N. MINCER and A. H. CLAUER, *J. Mater. Sci.* **20** (1985) 1873.

Received 14 April
and accepted 30 June 1986